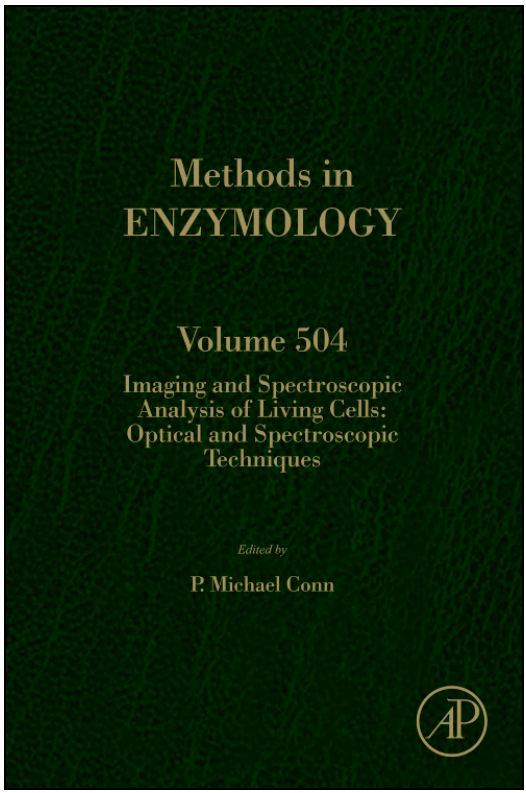

From: Jaideep Mathur, Sarah Griffiths, Kiah Barton, and Martin H. Schattat,
Green-to-Red Photoconvertible mEosFP-Aided Live Imaging in Plants.
In P. Michael Conn, editor: Methods in Enzymology, Vol. 504, Burlington:
Academic Press, 2012, pp. 163-181.
ISBN: 978-0-12-391857-4

CHAPTER EIGHT

Green-to-Red Photoconvertible mEosFP-Aided Live Imaging in Plants

Jaideep Mathur, Sarah Griffiths, Kiah Barton, *and* Martin H. Schattat

Contents

Abstract

Numerous subcellular-targeted probes have been created using a monomeric green-to-red photoconvertible Eos fluorescent protein for understanding the growth and development of plants. These probes can be used to create color-based differentiation between similar cells, differentially label organelle subpopulations, and track subcellular structures and their interactions. Both green and red fluorescent forms of mEosFP are stable and compatible with single colored FPs. Differential highlighting using mEosFP probes greatly increases spatiotemporal precision during live imaging.

Department of Molecular and Cellular Biology, Laboratory of Plant Development and Interactions, University of Guelph, Guelph, Canada

Methods in Enzymology, Volume 504
ISSN 0076-6879, DOI: 10.1016/B978-0-12-391857-4.00008-2

1. Introduction

Fluorescent proteins (FPs) are essential tools for understanding gene activity, protein localization, and subcellular interactions. Numerous subcellular-targeted FP probes have been created for live imaging of plants at the organ, tissue, cell, subcellular, and suborganelle levels (Mano *et al.*, 2008, 2011; Mathur, 2007; Mohanty *et al.*, 2009; Nelson *et al.*, 2007). The emission spectra of most commonly used FPs span discrete color bands (Shaner *et al.*, 2007). Consequently, all targets highlighted by a particular FP fusion display one color only. Single color labeling becomes a limiting factor when the aim of an experiment is to understand interactions between similar organelles. Limitations of using single color FPs also become apparent when trying to visualize highly localized and transient changes in the organization of dynamic subcellular elements like the cytoskeleton and the endomembrane system. Finally, most live-imaging techniques suffer from the absence of built-in controls in the cells under observation. For most researchers, the decision of when to stop imaging of a cell and avoid artifacts due to photoinduced damage remains an empirical decision that is not based on clear imaging parameters. In most studies of living cells, internal controls for subcellular damage are missing, and it is generally assumed that such effects must be negligible (Mathur *et al.*, 2010). However, as demonstrated recently (Schattat *et al.*, 2011; Sinclair *et al.*, 2009), plant cells respond rapidly and internal indicators are extremely important for minimizing artifacts while studying subcellular interactions.

"Optical highlighters" are recent additions to the FP toolbox. They are broadly categorized as photoactivable, photoswitchable, and photoconvertible (Ai *et al.*, 2006; Shaner *et al.*, 2007; Wiedenmann *et al.*, 2009). These proteins undergo structural changes in response to specific wavelengths that result in their "switching on" to a bright fluorescent state (e.g., photoactivable FPs; Patterson and Lippincott-Schwartz, 2002) or cause a shift in their fluorescence emission wavelength (photoconvertible FPs; Wiedenmann *et al.*, 2004; Gurskaya *et al.*, 2006). Photoswitchable proteins can switch back and forth between two states (Adam *et al.*, 2008). A number of photoconvertible proteins have been produced (Table 8.1). Among them EosFP, a homolog of Kaede derived from *Lobophyllia hemprichii* has been engineered to a monomeric form (mEosFP) without loss in fluorescence and photoconversion properties (Nienhaus *et al.*, 2005; Wiedenmann *et al.*, 2004). It has been used for demonstrating clathrin-dependent endocytosis during internalization of PIN auxin efflux carriers (Dhonukshe *et al.*, 2007), for labeling F-actin (Schenkel *et al.*, 2008) and peroxisomes (Sinclair *et al.*, 2009) in plants. In its unconverted form, mEosFP displays bright green fluorescence, while upon illumination with approximately 390–405 nm light, it changes rapidly into an irreversible red fluorescent form

Table 8.1 Useful photoconvertible probes

Protein	Color	Chromophore	Excitation peak (nm)	Emission peak (nm)	Brightness (m*M* cm)$^{-1}$	State	Reference
tdEos	Green	HYG	506	516	55	Tandem dimer	Nienhaus *et al.* (2006)
	Red		569	581	20		
EosFP WT	Green	HYG	506	516	50	Tetramer	Wiedenmann *et al.* (2004)
	Red		571	581	23		
mEosFP	Green	HYG	505	516	43	Monomer	Wiedenmann *et al.* (2004)
	Red		569	581	23		
mEosFP2	Green	HYG	506	519	47	Monomer	McKinney *et al.* (2009)
	Red		573	584	30		
Dendra2	Green	HYG	490	507	23	Monomer	Gurskaya *et al.* (2006)
	Red		553	573	19		
Kaede	Green	HYG	508	518	87	Tetramer	Ando *et al.* (2002)
	Red		572	580	20		
mKikGR	Green	HYG	505	515	34	Monomer	Habuchi *et al.* (2008)
	Red		580	591	18		
KikGR	Green	HYG	507	517	20	Tetramer	Tsutsui *et al.* (2005)
	Red		583	593	18		
mClavGR2	Green	HYG	488	504	34	Monomer	Hoi *et al.* (2010)
	Red		566	583	18		
mIrisFP	Green	HYG	486	516	NA	Monomer	Fuchs *et al.* (2010)
	Red		546	578			
IrisFP	Green	HYG	488	516	NA	Tetramer	Adam *et al.* (2008)
	Red		551	580			
PS-CFP	Cyan	SYG	400	468	9	Monomer	Chudakov *et al.* (2004)
	Green		490	511	11		

Information provided in the table is primarily based on Shaner *et al.* (2007) and Wiedenmann *et al.* (2004)

Table 8.2 mEosFP-based probes targeted to different subcellular compartments in plants

Name of probe Target compartment	Sequence used for targeting/basic reference
mEosFP-cytosolic cytosol	Nontargeted monomeric EosFP/Wiedenmann *et al.* (2004)
mEosFP::PIP1 plasma membrane	**At3g61430:** CDS plasma membrane intrinsic protein 1, ATPIP1/Fetter *et al.* (2004)
mEosFP:: α−TIP1 vacuolar membrane	**At1g73190:** CDS alpha tonoplast intrinsic protein/Hunter *et al.* (2007)
mEosFP::ER mem ER membrane	**At5g61790:** membrane targeting sequence of calnexin 1/Runions *et al.* (2006)
Mito-mEosFP mitochondria	First 261 bp of the *N. plumbaginifolia* mitochondrial ATP2-1/Logan and Leaver (2000)
mEosFP-2xFYVE endosomes/PVC	2X-FYVE domain from mouse HGF-regulated tyrosine kinase substrate protein/Voigt *et al.* (2005)
mEosFP::GONST1 Golgi bodies	**At2g13650:** CDS GONST 1/Baldwin *et al.* (2001)
mEosFP::PTS1 peroxisome matrix	C-terminal tripeptide "SKL" (PTS1)/Mathur *et al.* (2002); Sinclair *et al.* (2009)
mEosFP::MBD-MAP4 microtubules	Microtubule-binding domain of mammalian MAP-4/Marc *et al.* (1998)
LIFEACT::mEosFP F-actin	17 aa peptide from yeast Abp140p/Riedl *et al.* (2008)
mEosFP::FABD-mTn F-actin	F-actin binding domain of mammalian Talin/Kost *et al.* (1998); Schenkel *et al.* (2008)

(Table 8.1). EosFP does not mature optimally at 37 °C (McKinney *et al.*, 2009), but this limitation does not pose a major concern for its use in plants. Consequently, a number of mEosFP-based probes targeted to different components and compartments of the plant cell have been created (Mathur *et al.*, 2010; Table 8.2).

2. Expression of mEosFP Fusion Proteins in Plants

2.1. Transient expression

Transient expression of gene constructs provides a fast alternative to study the gene of interest in plant cells without generating stable transgenic lines, which is often much more laborious and time consuming. Depending on the purpose, the plant species under investigation, and available resources, the different transient expression methods for plants include transformation of protoplasts using polyethylene glycol (PEG; Mathur and Koncz, 1997) or electroporation (Bates, 1999), direct microinjection (Miki *et al.*, 1989), biolistic bombardment of gold or tungsten particles coated with DNA (Klein *et al.*, 1987), and Agrobacterium (Kim *et al.*, 2009; Wroblewski *et al.*, 2005; Wydro *et al.*, 2006) as well as virus-mediated gene expression (Scholthof *et al.*, 1996). For studying the behavior of FP fusion constructs, infiltration of plant tissue with *Agrobacterium tumefaciens* and biolistic bombardment are probably the most commonly used techniques. The routinely used method for transiently expressing mEosFP constructs and pertinent notes are as follows.

2.1.1. Agro-infilteration

Infiltration of leaf tissue of tobacco with *A. tumefaciens* does not require special or expensive equipment and results in very efficient transient expression of the introduced transgene.

2.1.1.1. Materials required

2.1.1.1.1. Plants

- About 6-week-old *Nicotiana benthamiana* plants, grown on soil in a short-day light cycle (8 h light/16 h dark; light intensity 80–100 μ mol m^{-2} s^{-1}) at 21 °C during day and 16 °C during night. (*Note*: *N. benthamiana* can also be grown under long-day conditions with higher temperatures but leaf plastids accumulate more starch under these conditions. Although different developmental stages, from seedlings to mature flowering plants can be utilized for infiltration, leaves from young plants generally result in higher transformation rates.)

2.1.1.1.2. Reagents

- *Agrobacterium* Infiltration Media (AIM) consists of 10 m*M* $MgCl_2$, 5 m*M* MES, pH 5.6, and 150 μM acetosyringone; for creating 50 ml AIM, mix 0.5 ml $MgCl_2$ (stock 0.5 *M*), 0.5 ml MES (stock 1 *M*), pH 5.6, and 7.5 μl acetosyringone (stock 1 *M* in DMSO). Add H_2O to make up the final volume of 50 ml (*Note*: AIM should not be stored at 4 °C for longer than 2 weeks).
- YEB medium liquid or solidified with agar in a Petri dish.

2.1.1.1.3. Material and disposals

- Cork borer, 1-ml needleless syringe, 1-ml pipette, sterile tips, 2-ml reaction tubes, glass culture tubes, gloves, marker pen.

2.1.1.2. Protocol

2.1.1.2.1. Before infilteration

- Use fresh *Agrobacterium* cultures. Incubate over night at 28 °C. (*Note*: *A. tumefaciens* grows significantly slower than *Escherichia coli* and starting a liquid culture from a single colony takes usually 2–3 days. If a 28 °C incubator is not available, *A. tumefaciens* cultures can also be grown at lower temperature (e.g., 22 ° C) but will need longer to reach the same density.)

2.1.1.2.2. Infilteration

- Harvest bacteria by spinning 2 ml of a liquid culture in a table-top micro centrifuge at 10,000 rpm for a minute discarding the supernatant. (*Note*: Bacteria can be harvested directly from a YEB plate too.) Resuspend bacteria in 1.5 ml AIM and incubate for 1–2 h at room temperature.
- Obtain an optical density of 0.8 at 600 nm. (*Note*: The expression level can be influenced by the amount of infiltrated cells, and the optimal OD_{600nm} might have to be evaluated and adjusted for each construct. Several different constructs can be coexpressed by mixing different *A. tumefaciens* cultures.)
- Perform the infiltration with a 1-ml needle-less syringe by gently pressing the syringe on the lower side of the leaf. Exert a counterpressure with a gloved finger on the other side of the leaf. Successful infiltration will be visible as a spreading dark green area. Mark its limits with a marker pen.

2.1.1.2.3. Postinfilteration

- Depending on the maturation time of the expressed protein and expression level, observations can usually be made 48–72 h after infiltration. Punch out a leaf disk by using a cork borer and observe the lower epidermis by epifluorescent or CLSM.

2.1.2. Biolistic bombardment

In comparison to the agro-infilteration method, the method involving coating of gold or tungsten particles with DNA is cumbersome, involves a proprietary biolistic particle delivery system (Bio-Rad PDS-1000/He; http://www.bio-rad.com/) and expensive consumables. The expression of mEosFP probes is usually assessed between 6 and 20 h after bombardment. This is a useful method if chlorophyll autofluorescence is a major impediment to observation since achlorophyllous cells such as those of the onion bulb epidermal layer can be used.

2.1.3. General notes

Great care must be taken in interpreting observations made using transient expression assays, since over a period of 6–90 h, the protein expression levels within a cell rise to a maximum and decline. Ideally, multiple observations spanning several hours should be taken since changes in protein expression levels invariably result in artifacts that may bias conclusion on subcellular localization and behavior. While not limited to mEosFP-based probes, certain endomembrane probes, such as CX-mEosFP (Table 8.2), tend to form aggregates or get sequestered into large brightly fluorescent vesicles. Overexpression of certain membrane-binding proteins such as the PI3P sensor mEosFP-2XFYVE appears to affect normal cellular functioning and generally increases the number of prevacuolar compartments within a cell (Mathur *et al.*, 2010; Vermeer *et al.*, 2006). Moreover, like monomeric GFP, nontargeted cytosolic mEosFP or its fusion with another small protein can diffuse freely in and out of the nucleus. For reasons that are unclear, over time the freely diffusing cytosolic mEosFP can become sequestered within the nucleus to suggest an artifactual nuclear localization pattern. Aggregates of mEosFP frequently appear as bright yellow-orange punctae and are easily visible in the 540–590 nm range even without photoconversion.

2.2. Creation of stable transgenic plants

A large number of plants can be transformed using *Agrobacterium* sps. to create stable transgenic lines. *Arabidopsis thaliana*, the model angiosperm, is easily transformed using the floral dip method (Clough and Bent, 1998). Although the creation of stable transgenics takes longer than transient assays, the availability of multiple lines provide the necessary range of observations that can point to phenotypic aberrations, specific tissue, cell, or subcellular pattern that might be associated with a probe. The availability of normally developing stable transgenic lines lends higher credibility to a particular probe for its use in cell biological observations. In our hands, the process (for *Arabidopsis*) usually requires up to 70 days.

2.2.1. Maintaining plants for experiments

Seeds from stably transformed Arabidopsis lines are grown on 1% agar-gelled Murashige and Skoog (1962) medium, supplemented with 3% sucrose, and with pH adjusted to 5.8. Plants are grown in Petri dishes in a growth chamber maintained at 21 ± 2 °C, and a 16/8 h light/dark regime using cool white light at approximately 80–100 μmol m^{-2} s^{-1}.

3. Visualization of mEosFP Probes in Plants

EosFP can be photoconverted from its green form (mEosFP-G) into a red fluorescent form (mEosFP-R) by a 405-nm wavelength centered violet-blue light. A diode 50 mW 405 nm violet laser is available and provides seamless functional coordination in both confocal and multiphoton microscopy systems under the control of pertinent software. However, for many laboratories, the addition of a 405-nm laser to an existing setup is not economically feasible. In such cases, a hybrid approach is advocated (see *Notes*).

3.1. Microscopy setup

- Any epifluorescent microscope equipped with a digital camera can be used for visualizing and gathering images from mEosFP-based probes. (*Note*: An epiflourescent microscopy setup with a digital camera is sufficient for visualizing and capturing images of EosFP probes. However, a confocal laser scanning microscope (CLSM) with 405, 488, 514, and 543 nm laser lines adds considerably to the clarity of images. CLSMs also provide a high degree of automation during photoconversion, image acquisition, and data processing.)
- Multipinhole iris diaphragm (*Note 2*: The hybrid approach involves carrying out the photoconversion step by using excitation wavelengths from glass filters (DAPI or D) followed by image acquisition using 488 and 543 nm laser scanning mode. In general, the broader bandwidth provided by glass filters is more efficient in carrying out the green-to-red photoconversion as compared to the 405-nm laser which is limited to the excitation peak for EosFP. The obvious limitation with the hybrid approach is the requirement for manually controlling the photoconversion process and thus missing the precision and automation that is possible through software-mediated control of the 405-nm laser. However, photoconversion via software control of laser positioning and scan time is best executed for large ROIs and for creating multiple ROIs in a sample. When dealing with motile approximately 1 μm diameter organelles such as mitochondria, peroxisomes, and Golgi bodies, the time between selection

of a target organelle and its photoconversion is generally long enough to allow the organelle to move away from the selected ROI. Thus, the limitation in creating a small ROI for photoconversion can be overcome partially by modifying the field iris diaphragm to obtain smaller pinholes. While diaphragms on standard microscopes contain aperture sizes distributed between 7 mm and 500 μm, most microscopy companies can create additional apertures upto 50 μm at relatively small cost).

- A high pressure mercury plasma arc-discharge lamp (e.g., Mercury Short ARC #HBO 103 W/2 (OSRAM GmbH, Steinerne Furt 62, 86167 Augsburg, Germany)).

3.1.1. Lens

- Standard lens (10×, 20×, 40×, 63×) for epifluorescent microscopy with the highest available numerical aperture are recommended.
- 40× and 63× water dipping lens recommended for live imaging. (*Note 3*: Ceramic-coated water-immersion lens with a long working distance are very convenient for visualizing living seedlings of *Arabidopsis*. Plants are mounted in deionized water on a depression slide and a coverslip (24 × 60 mm) placed on them while avoiding the air bubble formation. A drop of clean milli-Q water is placed on the coverslip and the lens dipped into it.)

3.1.2. Glass filter cubes

- DAPI/Hoechst/AMCA filter (Ex: 340–380; 400 DCLP; Em: 435–485 nm; Chroma Filter # 31000v2) or a "D" filter (excitation filter: 355–425 nm; dichromatic mirror 455 nm; suppression filter LP 470 nm). (*Note 4*: Photoconversion can be achieved using the DAPI filter commonly available on most epifluorescent microscopes). However, in living plant cells exposure to the UV wavelength from this filter causes a rapid increase in subcellular reactive oxygen species (ROS) and leads to photobleaching of both green and red forms of EosFP. We have found the narrower bandwidth "D" filter in combination with a high pressure mercury plasma arc-discharge lamp provides a violet-blue light optimal for use with plant cells. It minimizes exposure to harmful UV radiation while achieving maximum photoconversion. Depending upon the source and intensity of the light, an exposure time ranging from 2 to 10 s is sufficient for photoconversion.
- An Endow GFP bandpass emission filter (HQ 470/40X; Q 495/LP; HQ 525/50 m; Chroma Filter #41017)
- A TRITC (green) filter (HQ535/30x; Q570LP; HQ620/60 m; e.g., Chroma Filter # 41002c)

3.1.3. Material and disposals

- Glass slides (*Note*: Depression slides maintain plants in a moist condition and are very useful when using water-immersion lens.)
- Coverslips (premium glass 24 × 60 mm recommended for observing living plants)

3.2. General protocol for photoconversion

- Plant sample placed on microscope stage and area for visualization selected using the FITC filter. (*Note*: Plant cells should not be exposed to blue light for long as photobleaching occurs. If chloroplasts in a cell appear orange-yellow, choose another area for observing, as that region is already photodamaged. If a nonchlorophyllous cell looks yellow-green, the cell is displaying autofluorescence that might be due to drying or a mechanical damage. Roots of some plants exhibit green autofluorescence and should be checked beforehand.)
- A region of interest (ROI) brought into focus using appropriate iris aperture setting manually or by selecting appropriate software-mediated controls on CLSM.
- Image acquired using blue (FITC) and green (TRITC) filters on epi-fluorescent microscope or using 488 and 543 nm laser scanning on a CLSM. Only a green fluorescent image should be visible at this stage.
- Photoconversion for 3–10 s (or ROI scans in CLSM mode).
- Switch to TRITC filter for visualizing photoconverted ROI or on a CLSM switch to 488 and 543 nm laser-scanning mode for obtaining images in green and red channels simultaneously.
- Merge/overlay red and green images to observe photoconverted and non-photoconverted regions.
- Depending upon the experiment, build up image series in *xyz*, *xyt*, or *xyzt* dimensions.

3.3. Caveats

Whereas our knowledge of mEosFP functioning in plants is recent, certain relevant lessons learnt from *Arabidopsis* plants deserve special attention.

3.3.1. Unintentional photoconversion

Transgenic *Arabidopsis* plants expressing cytosolic mEosFP probes under a strong promoter often exhibit an artifact whereby the nuclei in some cells appear bright red even when the plants have not been photoconverted specifically. The probable reason for this artifact might be the presence of a 405-nm peak within the spectrum of white fluorescent lamps commonly used in plant growth chambers (Source: Spectral Power Distributions of

SYLVANIA; Fluorescent Lamps: OSRAM SYLVANIA USA, www.sylvania.com). The red photoconversion observed in the nuclei of old plants exposed to white light clearly differs from the yellow-orange emission observed from vesicles that have sequestered high concentrations of mEosFP fusions.

3.3.2. Partial photoconversion of mEosFP probes

The green form of mEosFP does not undergo photoconversion without violet-blue excitation, while the red photoconverted form does not revert to the green one. Thus, it is possible to have a variable mixture of green and red forms in an ROI. Hues ranging from green to red are created depending upon the exposure time and can be quite confusing if the experiment involves colocalization of proteins. Care must be taken to completely photoconvert mEosFP and ensure that minimal green fluorescence is observed in the ROI.

4. Uses of mEosFP Probes in Plants

The mEosFP probes (Table 8.2) are functional at different levels of plant organization and as shown in the following section can be used for a variety of purposes.

4.1. mEosFP for tracking organelles

Depending upon the size of the ROI selected for photoconversion, mEosFP probes can be used for differential color highlighting of tissues (e.g., for following lateral root development), a group of cells (e.g., for observing stomatal patterning in an expanding leaf), single cells (e.g., following changes in trichome or root hair position over time) (Fig. 8.1A), a subpopulation of organelles (e.g., dispersal of mitochondria from one subcellular region to another), a single organelle (e.g., tracking a single plastid during response to changing light conditions; Fig. 8.1B), and even suborganellar regions (e.g., observing changes in the location of nucleoli within the nucleus). The use of mEosFP probes for tracking is most effective when the probe is concentrated in a small organelle or vesicle and when it is not being constantly renewed through fresh protein turnover.

4.2. Tracking proteins from one compartment to another

Many proteins and lipids are moved between subcellular compartments for their modification or achieving a specific biochemical function. When fused to mEosFP, it is possible to photoconvert the proteins that are in the cytosol or sequestered in the ER-lumen and observe their progressive accumulation

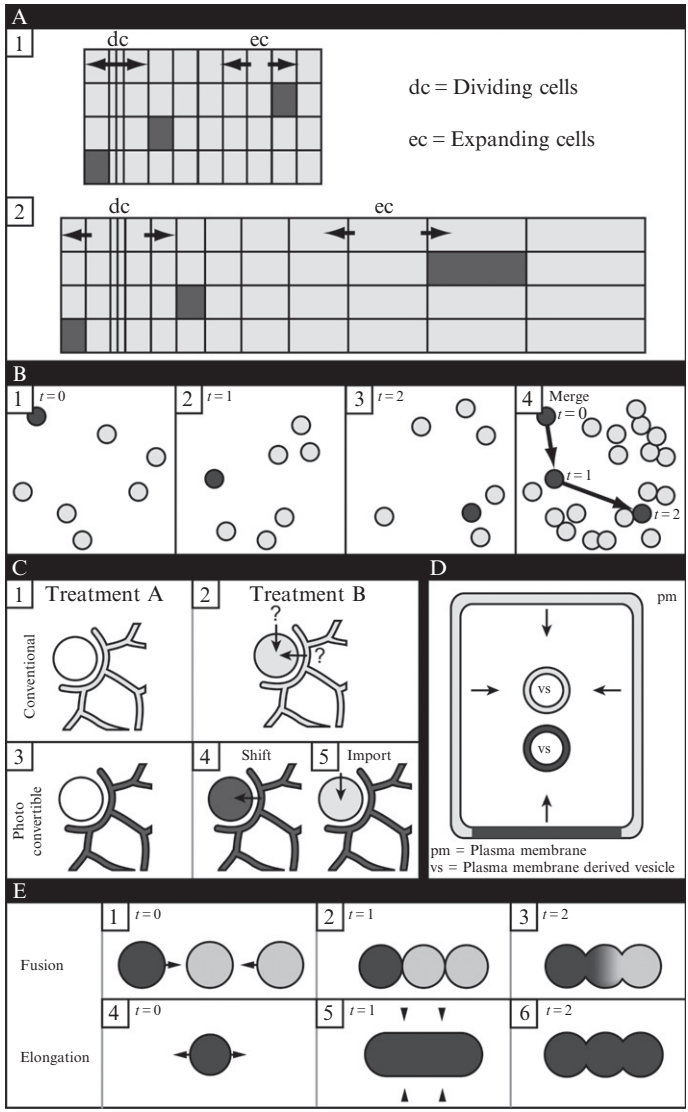

Figure 8.1 Diagrammatic depictions of use of mEosFP-based probes in plants. Fluorescent protein free areas are depicted in white; green fluorescent state is depicted in light gray, and the photoconverted red fluorescent state is shown as dark gray-black. (A) Tracking cells during development—cell division and cell expansion result in neighboring cells being shifted into relatively new positions. Photoconversion of mEosFP makes single cells easily recognizable within a population. The method works best for symplastically isolated cells and cell groups. (B) Tracking single organelles or a subpopulation of organelles—cytoplasmic streaming creates a complex mix of subcellular movements that makes it difficult to track a single organelle over time. Photoconversion using mEosFP (light gray dots in 1–4) creates color differentiation and allows long-term tracking using time-lapse imaging. The track of

in other compartments (Fig. 8.1C). Similarly, Eos-based probes have been used to track photoconverted vesicles from the plasma membrane into other regions of a cell (Dhonukshe *et al.*, 2007; Fig. 8.1D).

4.3. Using EosFP probes for understanding organelle fusion

As depicted in Fig. 8.1E, mEosFP probes can be used to demonstrate fusion between similar organelles (e.g., mitochondria; Arimura *et al.*, 2004) or provide compelling evidence for nonfusion of organelles like peroxisomes during their rapid elongation due to oxidative stress (Sinclair *et al.*, 2009).

4.4. Color recovery after photoconversion

A milder form of the FRAP (fluorescence recovery after photobleaching) technique is possible using mEosFP probes. FRAP is carried out by photobleaching an FP in an ROI with a strong pulse of the excitation wavelength. The recovery in fluorescent intensity increases over time as new fluorescent particles move into the bleached ROI until the prebleached state of fluorescence is reached (Fig. 8.2A). This information is used to calculate the diffusion coefficient for proteins under consideration (Axelrod *et al.*, 1976; Braga *et al.*, 2004). The FRAP procedure assumes that, although the light pulse is strong enough to bleach a fluorophore, it does not damage other molecules surrounding the ROI and in general does not interfere with cellular activity.

By contrast, the irreversible conversion of mEosFP from green to red allows observations on the dispersal of the red form and return of green fluorescence in an ROI after photoconversion. There is no dark

photoconverted organelles is recreated by simple maximum projection of a series of time-lapse images (dark gray dots in 1–4). (C) Tracking condition-dependent localization of proteins—many proteins exhibit condition-dependent localization to different subcellular compartments (depicted as treatment A (1, 3) and treatment B (2,4,5)). It is difficult to distinguish using conventional FPs (e.g., GFP; light gray in 1,2) whether the existing protein has shifted between compartments or if newly synthesized protein has been differentially targeted (2). Photoconversion of the protein before application of treatment B allows protein movement to be followed and the gradual localization of red fluorescence in another region. In case of newly synthesized and imported protein, the accumulation of unconverted green mEosFP rather than the red form would be observed. (D) Origin of membrane-derived vesicles—as demonstrated for Pin proteins (Dhonukshe *et al.*, 2007), mEosFP probes can be used to identify the origin of membrane-derived vesicles. Only vesicles derived from photoconverted areas exhibit the red fluorescence and can be tracked to other locations within the cell. (E) Morphological changes in organelles—fusion of organelles (1–3) and rapid organelle elongation (4–6) are frequently observed phenomena in living plant cells. Photoconversion-induced differential coloring of organelles is able to distinguish between fusion and membrane elongation events. Fusion results in organelles acquiring an intermediate color between the green and the red forms of mEosFP.

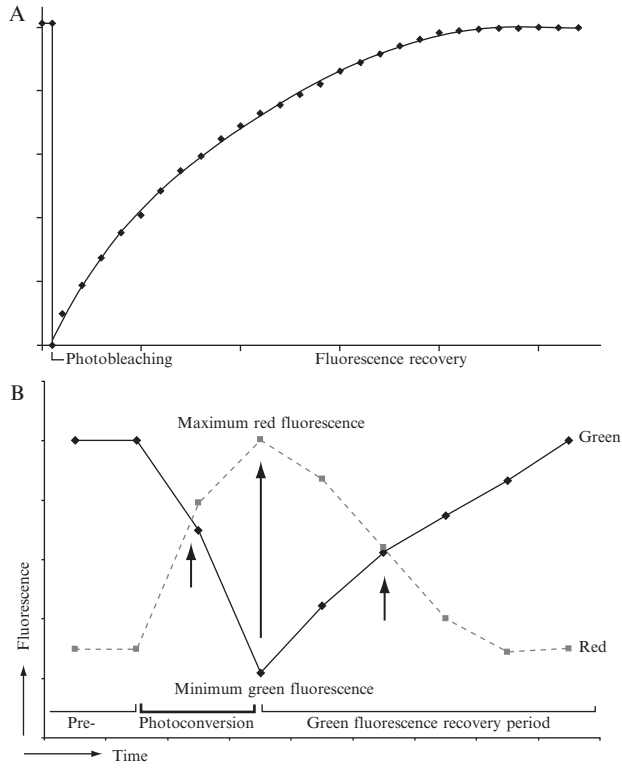

Figure 8.2 Typical representation of fluorescence values plotted against time for (A) fluorescence recovery after photobleaching (FRAP) and (B) color recovery after photoconversion (CRAP). Whereas photobleaching (A) results in a dark state in a region of interest photoconversion (B) brought about through a relatively mild excitation wavelength maintains a visible fluorescent state (green or red) throughout the experiment. The recovery curve for green fluorescence is dependent on the rate of movement of non-photobleached/non-photoconverted proteins from surrounding areas and is similar in both cases.

photobleached state and the red form provides visible proof of normal cellular functioning. Since after photoconversion, the intensity of the green fluorescence drops significantly, while the red form becomes predominant, the intensity of green as it recovers can be used in an identical manner to the way it would be used in a FRAP module. In many cases, FRAP is used in a qualitative manner, to determine whether diffusion is faster or slower compared to a control (Sprague *et al.*, 2004). For this purpose, color recovery of mEosFP after photoconversion can provide comparable recovery graphs with the difference that there is no steep drop to a photobleached dark state (Fig. 8.2A vs. B). Instead, the green fluorescent converts to a red fluorescent state. Both the green and the red form are visible, and the recovery graph from red back to the green state is comparable to the graph obtained through FRAP.

5. Post Acquisition Image Processing and Data Creation

The utility of mEosFP-based probes lies in their ability to become differentially colored. A wide variety of software tools are available for discriminating colors in an image. Many of the software that can be used for interpreting an image are available freely (e.g., ImageJ program, <http://rsb.info.nih.gov/ij> and its slightly enhanced distribution package version "Fiji" <http://mac.softpedia.com/get/Graphics/Fiji.shtml>). Most available software programs use the ICC compliant RGB triplet code for true colors as well as HTML-based Web applications code (Cowlishaw, 1985). Alternatively, the color picking tool and RGB value tables form integral components of commonly used digital coloring software such as Canvas and Adobe Photoshop. Table 8.3 lists a few useful plug-ins from the NIH public

Table 8.3 Some useful ImageJ plug-ins for image analysis of mEosFP probes

Plug-in	Description	URL
Color comparison	Color comparison of two 8-bit identically dimensioned gray scale images.	http://rsbweb.nih.gov/ij/plugins/color-comparison.html
RGB profiler	Draws the red, green, and blue profile plot of an image on the same plot, for each type of line selection (profile is refreshed).	http://rsbweb.nih.gov/ij/plugins/rgb-profiler.html
Color histogram	Generates a color histogram of RGB images.	http://rsbweb.nih.gov/ij/plugins/color-histogram.html
RGB measure	Separately measures the red, green, and blue channels of an RGB image.	http://rsbweb.nih.gov/ij/plugins/rgb-measure.html
RGB measure plus	Separately measures the red, green, and blue channels of an RGB image between user-defined threshold levels per channel. Should be combined with the threshold color plug-in.	http://rsbweb.nih.gov/ij/plugins/rgb-measure-plus.html

(*Continued*)

Table 8.3 (*Continued*)

Plug-in	Description	URL
Threshold color	Allows thresholding of color RGB images space.	http://www.dentistry.bham.ac.uk/landinig/software/software.html
Color profiler	Provides the same functionality as the Analyze/Plot Profile command but for RGB images.	http://rsbweb.nih.gov/ij/plugins/color-profiler.html
Interactive 3D surface plot	Creates interactive surface plots from all image types. Nonrectangular selections are supported.	http://rsbweb.nih.gov/ij/plugins/surface-plot-3d.html
RGB profile plot	Draws the red, green, and blue profile plot of an RGB image on the same Plot.	Comes with ImageJ
Color inspector	This plug-in shows the color distribution within a 3D-color space.	http://rsbweb.nih.gov/ij/plugins/color-inspector.html

domain funded ImageJ program. These tools allow breakdown of an image into red–green–blue values, creation of line traces, histograms, and 3D renditions that are useful for data presentation. Since protein levels are not really estimated, the programs mainly provide a qualitative comparison of ROIs in an image. However, with proper controls and through fluorescence comparisons with absolute green and red values on a 0- to 255-scale, ratiometric quantification can be achieved.

ACKNOWLEDGMENTS

We thank Joerg Wiedenmann for providing us the Eos FP. J. M. gratefully acknowledges funding from the Natural Sciences and Engineering Research Council of Canada (NSERC), the Canada Foundation for Innovation (CFI), the Ministry of Research and Innovation, Ontario, and the Keefer Trust, University of Guelph.

REFERENCES

Adam, V., Lelimousin, M., Boehme, S., Desfonds, G., Nienhaus, K., Field, M. J., Wiedenmaan, J., McSweeney, S., Nienhaus, G. U., and Bourgeois, D. (2008). Structural characterization of IrisFP, an optical highlighter undergoing multiple photo-induced transformations. *Proc. Natl. Acad. Sci. USA* **105**(47), 18343–18348.

Ai, H., Henderson, J. N., Remington, S. J., and Campbell, R. E. (2006). Directed evolution of a monomeric, bright and photostable version of *Clavularia* cyan fluorescent protein: Structural characterization and applications in fluorescence imaging. *Biochem. J.* **400,** 531–540.

Ando, R., Hama, H., Yamamoto-Hino, M., Mizuno, H., and Miyawaki, A. (2002). An optical marker based on the UV-induced green-to-red photoconversion of a fluorescent protein. *Proc. Natl. Acad. Sci. USA* **99,** 12651–12656.

Arimura, S., Yamamoto, J., Aida, G. P., Nakazono, M., and Tsutsumi, N. (2004). Frequent fusion and fission of plant mitochondria with unequal nucleoid distribution. *Proc. Natl. Acad. Sci. USA* **101,** 7805–7808.

Axelrod, D., Koppel, D. E., Schlessinger, J., Elson, E., and Webb, W. W. (1976). Mobility measurement by analysis of fluorescence photobleaching recovery kinetics. *Biophys. J.* **16,** 1055–1069.

Baldwin, T. C., Handford, M. G., Yuseff, M. I., Orellana, A., and Dupree, P. (2001). Identification and characterization of *GONST1*, a golgi-localized GDP-mannose transporter in Arabidopsis. *Plant Cell* **13,** 2283–2295.

Bates, G. W. (1999). Plant transformation via protoplast electroporation. *Plant Cell Cult. Protoc.* **111,** 359–366.

Braga, J., Desteroo, J. M. P., and Carmo-Fonseca, M. (2004). Intracellular macromolecular mobility measured by fluorescence recovery after photobleaching with confocal laser scanning microscopes. *Mol. Biol. Cell* **15,** 4749–4760.

Chudakov, D. M., Verkhusha, V. V., Staroverov, D. B., Souslova, E. A., Lukyanov, S., and Lukyanov, K. A. (2004). Photoswitchable cyan fluorescent protein for protein tracking. *Nat. Biotechnol.* **22**(11), 1435–1439.

Clough, S. J., and Bent, A. F. (1998). Floral dip: A simplified method for *Agrobacterium*-mediated transformation of *Arabidopsis thaliana*. *Plant J.* **16,** 735–743.

Cowlishaw, M. F. (1985). Fundamental requirements for picture presentation. *Proc. Soc. Inform. Display* **26,** 101–107.

Dhonukshe, P., Aniento, F., Hwang, I., Robinson, D. G., Mravec, J., Stierhof, Y., and Friml, J. (2007). Clathrin-mediated constitutive endocytosis of PIN auxin efflux carriers in *Arabidopsis*. *Curr. Biol.* **17,** 520–527.

Fetter, K., Van Wilder, V., Moshelion, M., and Chaumont, F. (2004). Interactions between plasma membrane aquaporins modulate their water channel activity. *Plant Cell* **16,** 215–228.

Fuchs, J., Böhme, S., Oswald, F., Hedde, P. N., Krause, M., Wiedenmaan, J., and Nienhaus, G. U. (2010). A photoactivatable marker protein for pulse-chase imaging with superresolution. *Nat. Methods* **7**(8), 627–630.

Gurskaya, N. G., Verkhusha, V. V., Shcheglov, A. S., Staroverov, D. B., Chepurnykh, T. V., Fradkov, A. F., Lukyanov, S., and Lukyanov, K. A. (2006). Engineering of a monomeric green-to-red photoactivatable fluorescent protein induced by blue light. *Nat. Biotechnol.* **24,** 461–465.

Habuchi, S., Tsutsui, H., Kochaniak, A. B., Miyawaki, A., and Van Oijen, A. M. (2008). mKikGR, a monomeric photoswitchable florescent protein. *PLoS One* **3**(12), e3394.

Hoi, H., Shaner, N. C., Davidson, M. W., Cairo, C. W., Wang, J., and Campbell, R. E. (2010). A monomeric photoconvertible fluorescent protein for imaging of dynamic protein localization. *J. Mol. Biol.* **410,** 776–791.

Hunter, P. R., Craddock, C. P., Di Benedetto, S., Roberts, L. M., and Frigerio, L. (2007). Fluorescent reporter proteins for the tonoplast and the vacuolar lumen identify a single vacuolar compartment in Arabidopsis cells. *Plant Physiol.* **145,** 1371–1382.

Kim, M. J., Baek, K., and Park, C. M. (2009). Optimization of conditions for transient Agrobacterium-mediated gene expression assays in Arabidopsis. *Plant Cell Rep.* **28,** 1159–1167.

Klein, T. M., Wolf, E. D., Wu, R., and Sanford, J. C. (1987). High-velocity microprojectiles for delivering nucleic-acids into living cells. *Nature* **327,** 70–73.

Kost, B., Spielhofer, P., and Chua, N. H. (1998). A GFP-mouse talin fusion protein labels plant actin filaments in vivo and visualizes the actin cytoskeleton in growing pollen tubes. *Plant J.* **16,** 393–401.

Logan, D. C., and Leaver, C. J. (2000). Mitochondria-targeted GFP highlights the heterogeneity of mitochondrial shape, size and movement within living plant cells. *J. Exp. Bot.* **51,** 865–871.

Mano, S., Miwa, T., Nishikawa, S., Mimura, T., and Nishimura, M. (2008). The plant organelles database (PODB): A collection of visualized plant organelles and protocols for plant organelle research. *Nucleic Acids Res.* **36,** D929–D937.

Mano, S., Miwa, T., Nishikawa, S., Mimura, T., and Nishimura, M. (2011). The Plant Organelles Database 2 (PODB2): An updated resource containing movie data of plant organelle dynamics. *Plant Cell Physiol.* **52,** 244–253.

Marc, J., Granger, C. L., Brincat, J., Fisher, D. D., Kao, T. H., McCubbin, A. G., and Cyr, R. J. (1998). A GFP-MAP4 reporter gene for visualizing cortical microtubule rearrangements in living epidermal cells. *Plant Cell* **10,** 1927–1940.

Mathur, J. (2007). The illuminated plant cell. *Trends Plant Sci.* **12,** 506–513.

Mathur, J., and Koncz, C. (1997). PEG-mediated protoplast transformation with naked DNA. *Methods Mol. Biol.* **82,** 267–276.

Mathur, J., Mathur, N., and Hülskamp, M. (2002). Simultaneous visualization of peroxisomes and cytoskeletal elements reveals actin and not microtubule-based peroxisome motility in plants. *Plant Physiol.* **128,** 1031–1045.

Mathur, J., Radhamony, R., Sinclair, A. M., Donoso, A., Dunn, N., Roach, E., Radford, D., Mohaghegh, P. S., Logan, D. C., Kokolic, K., and Mathur, N. (2010). mEosFP-based green-to-red photoconvertible subcellular probes for plants. *Plant Physiol.* **154**(4), 1573–1587.

McKinney, S. A., Murphy, C. S., Hazelwood, K. L., Davidson, M. W., and Looger, L. L. (2009). A bright and photostable photoconvertible florescent protein for fusion tags. *Nat. Methods* **6**(2), 131–133.

Miki, B., Huang, B., Bird, S., Kemble, R., Simmonds, D., and Keller, W. (1989). A procedure for the microinjection of plant cells and protoplasts. *Methods Cell Sci.* **12,** 139–144.

Mohanty, A., Luo, A., DeBlasio, S., Ling, X., Yang, Y., Tuthill, D. E., Williams, K. E., Hill, D., Zadrozny, T., Chan, A., Sylvester, A. W., and Jackson, D. (2009). Advancing cell biology and functional genomics in maize using fluorescent protein-tagged lines. *Plant Physiol.* **149,** 601–605.

Murashige, T., and Skoog, F. (1962). A revised medium for rapid growth and bio assays with tobacco tissue cultures. *Physiol. Plant.* **15,** 473–497.

Nelson, B. K., Cai, X., and Nebenführ, A. (2007). A multi-color set of in vivo organelle markers for colocalization studies in Arabidopsis and other plants. *Plant J.* **51,** 1126–1136.

Nienhaus, K., Nienhaus, G. U., Wiedenmann, J., and Nar, H. (2005). Structural basis for photo-induced protein cleavage and green-to-red conversion of fluorescent protein EosFP. *Proc. Natl. Acad. Sci. USA* **102,** 9156–9159.

Nienhaus, G. U., Nienhaus, K., Holzle, A., Ivanchenko, S., Red, R., Oswald, F., Wolff, M., Schmitt, F., Rocker, C., Vallone, B., Weidemann, W., Heilker, R., *et al.* (2006). Photoconvertible fluorescent protein EosFP: Biophysical properties and cell biology applications. *Photochem. Photobiol.* **82,** 351–358.

Patterson, G. H., and Lippincott-Schwartz, J. (2002). A photo-activatable GFP for selective photolabeling of proteins and cells. *Science* **297,** 1873–1877.

Riedl, J., Crevenna, A. H., Kessenbrock, K., Yu, J. H., Neukirchen, D., Bista, M., Bradke, F., Jenne, D., Holak, T. A., Werb, Z., Sixt, M., and Wedlich-Soldner, R. (2008). Lifeact: A versatile marker to visualize F-actin. *Nat. Methods* **5,** 605–607.

Runions, J., Brach, T., Kühner, S., and Hawes, C. (2006). Photoactivation of GFP reveals protein dynamics within the endoplasmic reticulum membrane. *J. Exp. Bot.* **57,** 43–50.

Schattat, M., Barton, K., Baudisch, B., Klösgen, R. B., and Mathur, J. (2011). Plastid stromule branching coincides with contiguous endoplasmic reticulum dynamics. *Plant Physiol.* **155,** 1667–1677.

Schenkel, M., Sinclair, A. M., Johnstone, D., Bewley, J. D., and Mathur, J. (2008). Visualizing the actin cytoskeleton in living plant cells using a photo-convertible mEos:: FABD-mTn fluorescent fusion protein. *Plant Methods* **4,** 21.

Scholthof, H. B., Scholthof, K. B. G., and Jackson, A. O. (1996). Plant virus gene vectors for transient expression of foreign proteins in plants. *Annu. Rev. Phytopathol.* **34,** 299–323.

Shaner, N. C., Patterson, G. H., and Davidson, M. W. (2007). Advances in fluorescent protein technology. *J. Cell Sci.* **120,** 4247–4260.

Sinclair, A. M., Trobacher, C. P., Mathur, N., Greenwood, J. S., and Mathur, J. (2009). Peroxule extension over ER-defined paths constitutes a rapid subcellular response to hydroxyl stress. *Plant J.* **59,** 231–242.

Sprague, B. L., Pego, R. L., Stavreva, D. A., and McNally, J. G. (2004). Analysis of binding reactions by fluorescence recovery after photobleaching. *Biophys. J.* **86,** 3473–3495.

Tsutsui, H., Karasawa, S., Shimizu, H., Nukina, N., and Miyawaki, A. (2005). Semi-rational engineering of a coral fluorescent protein into an efficient highlighter. *EMBO Rep.* **6,** 233–238.

Vermeer, J. E., van Leeuwen, W., Tobeña-Santamaria, R., Laxalt, A. M., Jones, D. R., Divecha, N., Gadella, T. W., Jr., and Munnik, T. (2006). Visualization of PtdIns3P dynamics in living plant cells. *Plant J.* **47,** 687–700.

Voigt, B., Timmers, A. C., Samaj, J., Hlavacka, A., Ueda, T., Preuss, M., Nielsen, E., Mathur, J., Emans, N., Stenmark, H., Nakano, A., Baluska, F., *et al.* (2005). Actin-based motility of endosomes is linked to the polar tip growth of root hairs. *Eur. J. Cell Biol.* **84,** 609–621.

Wiedenmann, J., Ivanchenko, S., Oswald, F., Schmitt, F., Röcker, C., Salih, A., Spindler, K., and Nienhaus, G. U. (2004). EosFP, a fluorescent marker protein with UV-inducible green-to-red fluorescence conversion. *Proc. Natl. Acad. Sci. USA* **101,** 15905–15910.

Wiedenmann, J., Oswald, F., and Nienhaus, G. U. (2009). Fluorescent proteins for live cell imaging: Opportunities, limitations, and challenges. *IUBMB Life* **61,** 1029–1042.

Wroblewski, T., Tomczak, A., and Michelmore, R. (2005). Optimization of Agrobacterium-mediated transient assays of gene expression in lettuce, tomato and Arabidopsis. *Plant Biotechnol. J.* **3,** 259–273.

Wydro, M., Kozubek, E., and Lehmann, P. (2006). Optimization of transient Agrobacterium-mediated gene expression system in leaves of *Nicotiana benthamiana*. *Acta Biochim. Pol.* **53,** 289–298.